International Conference on Nuclear Data for Science and Technology 2007
DOI: 10.1051/ndata:07364

A new high efficiency array of C_6D_6 detectors for capture cross section measurements at GELINA

C. Sage[1,a], E. Berthoumieux[2], O. Bouland[3], F. Gunsing[2], A.J.M. Plompen[1], P. Schillebeeckx[1], P. Siegler[1], N. van Opstal[4], and R. Wynants[1]

[1] JRC, IRMM, Neutron Physics Unit, 2440 Geel, Belgium
[2] CEA Saclay, DSM/DAPNIA/SPhN, 91191 Gif-sur-Yvette, France
[3] CEA Cadarache, DEN/CAD/DER/SPRC/LEPh, 13108 Saint-Paul-lez-Durance, France
[4] XIOS, Hogeschool Limburg, 3590 Diepenbeek, Belgium

Abstract. Neutron capture cross section measurements at the **G**eel **E**lectron **Lin**ear **A**ccelerator (GELINA) rely on the use of H-free deuterated benzene C_6D_6 liquid scintillators. A new design of Aluminium canned C_6D_6 detectors was studied to improve the performances (high gamma efficiency vs. low neutron sensitivity) of the cylindrical previous ones: on the basis of a truncated 5-sides pyramid, the new detectors were developed and tested in Geel, and used in a preliminary capture cross section measurement on ^{197}Au in a 4 detectors setup.

1 Introduction

Capture cross section measurements at GELINA rely on the total energy detection principle. This implies the use of detectors with a low gamma-ray detection efficiency ($\varepsilon_\gamma \ll 1$) and an efficiency that is proportional to the gamma-ray energy ($\varepsilon_\gamma = kE_\gamma$).

Thus, an efficiency for a capture event is obtained that is independent of the decay cascade and hence of the resonance. The required proportionality is obtained by applying the pulse height weighting technique by means of the so-called weighting function $WF(E_d)$. The response function of the detection system $R_d(E_d,E_\gamma)$ is mathematically manipulated to achieve the proportionality between the detection efficiency and the gamma-ray energy. This technique is based on an original suggestion by Maier-Leibnitz which was first applied by Macklin and Gibbons [1] and fully explained in Ref [2].

At GELINA neutron induced capture reaction cross section measurements are performed at three measurements stations (L = 10, 30, 60 m) using a set of 2 or 4 C_6D_6 detectors. Hydrogen-free deuterated benzene scintillators have the great advantage of very low neutron sensitivity combined with good timing characteristics. However, for the study of enriched and radioactive isotopes, it was found that we need to maximize the detection efficiency in order to cover a wider range of cases with interest to various applications and users. Therefore, an array using up to 10 new C_6D_6 detectors is being constructed, combining a very low sensitivity to neutrons with a substantial increase of the detection efficiency. These new detectors benefit from a new design of Aluminium containers on the basis of a truncated 5-sides pyramid. The TEFLON tube surrounding the scintillator cell for its thermal expansion was replaced by an Aluminium half-ring on the back of the Aluminium container. This new shape implies the increase of the C_6D_6 volume by a factor 4, with a corresponding increase of the gamma ray detection efficiency.

[a] Presenting author, e-mail: christophe.sage@ec.europa.eu

Effective use of the array requires a precise characterisation of its detectors and of the array as a whole, for both gamma ray and neutron sensitivity. Here, results of Monte Carlo simulations using MCNP will be shown in comparison with measured responses using calibration sources and test measurements at GELINA.

2 Detector geometry modelling

The first step is the careful transcription of the detector geometry for the simulation code. A detector is composed of 2 parts: a 2.8L Aluminium container filled with C_6D_6 and an EMI9823KQ photomultiplier connected to it through a boron free quartz window. The Al container is a truncated 5-sides 12.5 cm high pyramid. A μ-metal shield covers the PM to provide an electromagnetic insulation. Deuterated benzene with a D:H ratio of 114 was used as scintillator material.

Figure 1 shows the modelled geometry as designed in the MCNP input file, using the VisEd 3D viewer included in the MCNP5 package [3,4], along with the same geometry modelled by means of the GEANT IV software. This figure shows up to which details the detectors were modelled in the simulations, and especially the design of the PM including the cylindrical glass tube with its several sections and the metal dynodes.

3 Simulated detector responses

3.1 Gamma efficiency

For MCNP simulations, we used the F8 pulse height tally to track photon and electron interactions along the path of the photon emitted by a monoenergetic point source placed at 9 cm from the detector [3]. An event was considered as detected if the calculated energy deposition in the scintillators was exceeding a threshold of 150 keV. The integral of deposited energy normalized to the quantity of incident energy

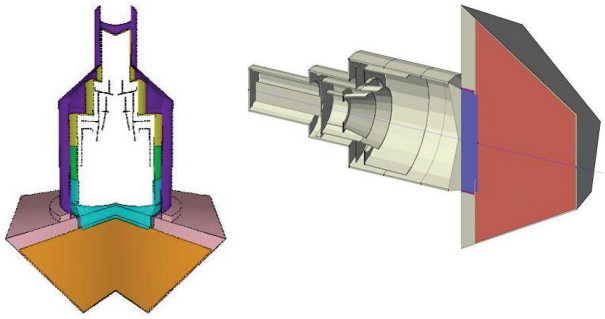

Fig. 1. C_6D_6 detector geometry as modelled in the MCNP and GEANT input files.

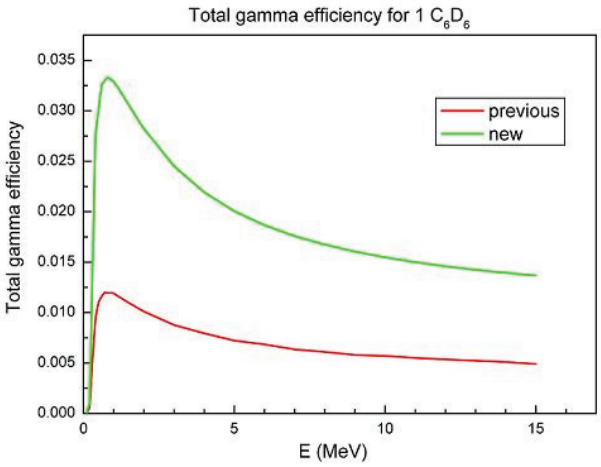

Fig. 2. Total gamma-ray efficiency for 1 detector.

defines the total gamma efficiency for one precise energy $\varepsilon_\gamma(E_\gamma)$.

$$\int R(E_d, E_\gamma) dE_d = \varepsilon_\gamma(E_\gamma). \quad (1)$$

The curve in figure 2 was obtained from calculations of this value for different monoenergetic point sources from 200 keV to 15 MeV. We observed that the ratio new/previous for the total gamma efficiency is a bit less than the expected value of 4, coming from the ratio of the scintillators volume in the new and the previous detectors. Besides, we can also notice that the gamma efficiency is definitively not proportional to the incident energy, which confirms the need of the weighing function described before.

3.2 Neutron sensitivity

The neutron sensitivity of C_6D_6 detectors, which is defined as the probability that a neutron entering the assembly creates a signal relative to the gamma-ray detection probability, is an important source of background. The consequences of this background, mainly coming from the neutron scattering in the sample, have been illustrated by Koehler et al. [5] in the example of a high resolution TOF measurement on ^{88}Sr, and further investigated by Plag et al. [6], who discussed in detail the various components contributing to the neutron sensitivity and reported on a C_6D_6 detector with the lowest

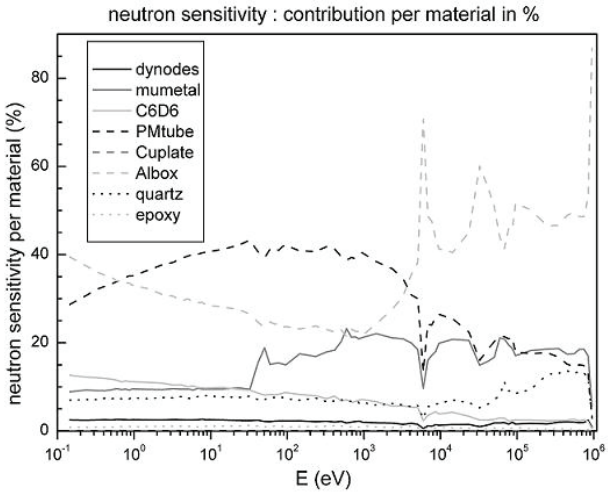

Fig. 3. Relative contribution of each component material to the detector neutron sensitivity.

neutron sensitivity that has ever been achieved. A. Borella et al. benchmarked the entire device in ref. [2]. This sensitivity of the detection system to neutrons plays indeed an important role for all resonances with a neutron width much larger than the radiation width, which is the case for light nuclei and for heavier nuclei close to shell closures.

We used the same tally for the MCNP simulations as for the gamma efficiency calculations, tracking the photon and electron interactions along the path of the neutron emitted from a point source. We also kept the minimum threshold of 150 keV to define a detected event in the scintillators. We simulated several monoenergetic neutron sources covering the energy range from 0.1 eV to 1 MeV (cf. ref. [7] for details of this neutron source description). Each detector response, consisting in the distribution of the energy deposited in the scintillators, was integrated and normalized to the detection probability for a 4 MeV gamma ray, so as to get the neutron sensitivity $\varepsilon_n/\varepsilon_\gamma$ [2,6].

Figure 3 shows the relative contribution of the different components as a function of neutron energy. This illustrates the strong impact of materials such as the 1 mm thick μ-metal shielding and the presence of ^{10}B fraction in the glass tube of the PM at low energies. The 5.9 keV and 35 keV Aluminium resonances are also strongly visible in the neutron sensitivity. The inelastic scattering threshold for Aluminium is responsible for the significant raise in its contribution at 1 MeV neutron energy.

Figure 4 compares the neutron sensitivity of the previous and the new geometry for one detector placed in a 4 detectors setup. We observe that these neutron sensitivities are of the same order of magnitude. Thus the improvement of the gamma efficiency by a factor 4 was not accompanied by an increase of the neutron sensitivity. Moreover, the contribution of Fluorine present in the TEFLON of the previous detector has disappeared, as can be seen with the lower neutron sensitivity above 100 keV for the new detector. The new detection system on the whole also seems to be less sensible to components resonance structures, as we can observe with the lack of resonance structure in the spectrum concerning the 45 eV and 131.4 eV Molybdenum resonances, as long with its other resonances

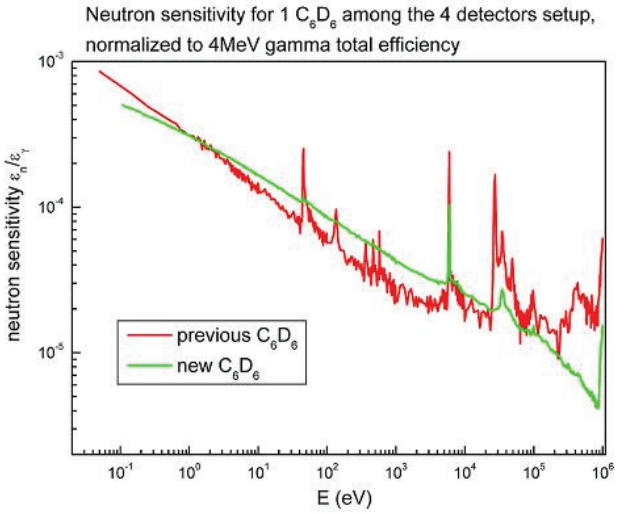

Fig. 4. Simulated neutron sensitivity for 1 detector among the 4 detectors setup.

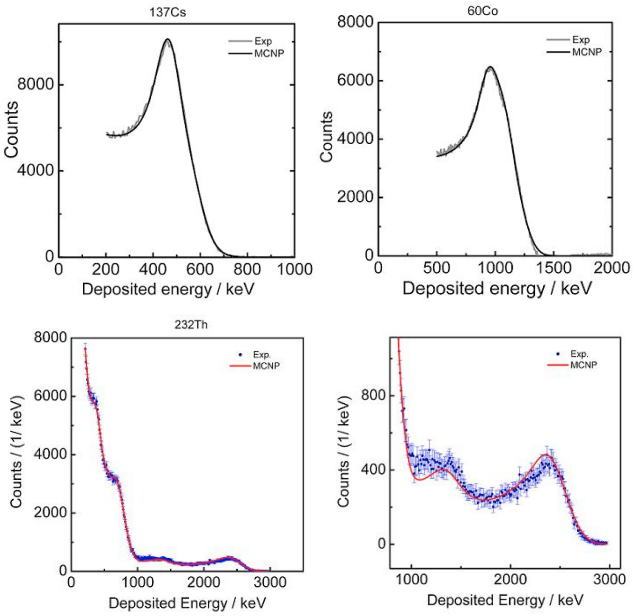

Fig. 5. Comparison of the simulation with measurements. 3 gamma ray calibration sources were measured: ^{137}Cs (661 keV), ^{60}Co (1.17 and 1.33 MeV), and the ^{232}Th decay chain gamma lines, the last curve showing a zoom from the higher energy part of the ^{232}Th spectrum.

between 300 and 700 eV. This is partially explained by the fact that the Molybdenum is only present in the μ-metal composition, and the shielding of the new detector is slightly smaller (10% less in terms of volume).

4 Comparison simulation/experiment

The experimental measurements were performed for a capture detection setup installed at the 10 m station at GELINA and consisting of 4 C_6D_6 detectors. The final response was obtained by a convolution of the simulated response $R_e(E_e,E_\gamma)$ with a Gaussian function G representing the amplitude

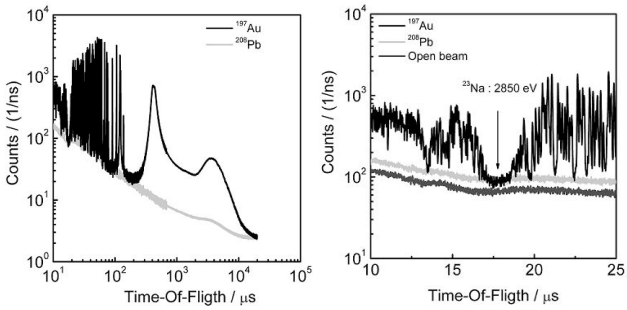

Fig. 6. ^{197}Au(n,γ) capture cross section measurement at the 10 m station, with a zoom at the ^{23}Na 2.85 keV black resonance.

resolution of the detector [2]:

$$R_d\left(\mathrm{E}_d, E_\gamma\right) = \int R_e\left(E_e, E_\gamma\right) G\left(E_d - \mu\left(E_e\right)\right) dE_e \qquad (2)$$

with

$$G\left(E_d - \mu\left(E_e\right)\right) = \frac{1}{\sqrt{2\pi}\sigma_\mu} \exp\left(-\frac{\left(E_d - \mu\left(E_e\right)\right)^2}{2\sigma_\mu^2}\right). \qquad (3)$$

In equation (2) the simulated response $R_e(E_e,E_\gamma)$ represents the transfer of gamma-ray energy E_γ in energy E_e which is deposited within the detector. The conversion of the energy E_e into the observed energy E_d is defined by the relationship $\mu(E_e)$ and a resolution broadening σ_μ, which are functional forms of E_e and $\mu(E_e)$, respectively. Ideally, $\mu(E_e)$ and σ_μ^2 are directly proportional to the energy E_e. To determine the functional relationships of the mean value and the variance together with the free parameters a similar procedure as discussed in ref. [8] was applied. The experimental response for well-known monoenergetic gamma-rays was compared with the simulated ones obtained from the combination of equations (2) and (3). The free parameters in the expressions for $\mu(E_e)$ and $\sigma^2(E_e)$ were determined by a least squares fitting procedure using experimental observed response functions. In order to determine the functional forms, it is sufficient to fit the upper portion of the measured spectrum.

The experimental response for monoenergetic gamma ray calibration sources such as ^{137}Cs (661 keV) and ^{60}Co (1.17 and 1.33 MeV) were compared with the simulated ones. We also compared the measurement of gamma rays from the ^{232}Th decay chain to the simulation, where the gamma lines from ref. [9] were used with their respective emission probabilities. We observed a very good matching for these 3 cases in the whole energy region, which indicates that the absolute detection efficiency in the high energy is very well reproduced by the simulations.

5 Preliminary results: application for capture cross section measurements

The first measurements with the setup of 4 new detectors were performed on a ^{197}Au sample at the 10 m station. The TOF of the neutron creating the capture event is recorded together with the energy deposited in the scintillators by the gamma ray.

The preliminary result shown in figure 6 also demonstrates the very good time resolution of the new C_6D_6 detectors. The close number of counts between open beam measurements and with the ^{197}Au and ^{206}Pb samples for the ^{23}Na black resonance confirms the low influence of the neutron sensitivity for these new detectors. Indeed, this latter being mainly due to the neutron scattering in the sample, it is therefore not present in an open beam measurement.

6 Outlook

The capture cross section measurement setup running at GELINA is undergoing an upgrade. The new C_6D_6 detectors, based on a new truncated pyramid geometry, have been installed in a 4 detectors array to perform preliminary calibration test and measurements in order to compare their characteristics with Monte Carlo simulations. The simulations concerning total gamma efficiency and neutron sensitivity demonstrated the improved performance, with a neutron sensitivity identical to the one of the previous detectors, but a gamma efficiency 3 times higher.

Moreover a very good matching concerning the response to monoenergetic gamma calibration sources was achieved.

In a next step experimental evaluations of the neutron sensitivity will be performed, along with simulations including the sample geometry. This will result in the calculation of the appropriate weighting functions for the detectors.

References

1. R.L. Macklin, J.H. Gibbons, Phys. Rev. **159**, 1007 (1967).
2. A. Borella, G. Aerts, F. Gunsing, M. Moxon, P. Schillebeeckx, R. Wynants, Nucl. Instrum. Meth. (accepted for publication).
3. X-5 Monte Carlo Team, *MCNP – A general Monte Carlo NParticle Transport Code, Version 5* (Los Alamos National Laboratory, New Mexico, April 24, 2003).
4. L.L. Carter, R.A. Schwarz, *MCNP Visual Editor Computer Code Manual* (Los Alamos National Laboratory, New Mexico, 2002).
5. P.E. Koehler et al., Phys. Rev. C **62**, 055803-1-15 (2000).
6. R. Plag et al., Nucl. Instrum. Meth. A **496**, 425 (2003).
7. G. Aerts, Ph.D. thesis, University of Paris XI, 2005, p. 67.
8. M. Weyrauch et al., Nucl. Instrum. Meth. A **405**, 442 (1998).
9. W.J. Lin, G. Harbottle, J. Radioanal. Nucl. Chem. **157**(2), 367 (1992).